Invited Paper

High Resolution Microlithography Applications of Deep-UV Excimer Lasers

F.K. Tittel[1], M. Erdélyi[2], G. Szabó[2], Zs. Bor[2], J. Cavallaro[1], and M.C. Smayling[3]

[1]Department of Electrical and Computer Engineering and Rice Quantum Institute, Rice University, 6100 Main, Houston, TX 77005-1892, USA

[2]Department of Optics and Quantum Electronics, JATE University, H-6720, Szeged, Dom ter 9, Hungary

[3]Texas Instruments, Inc., 12201 S.W. Freeway, MS 735, Stafford, TX 77477, USA

1. Introduction

The recent trend in microelectronics towards patterning critical feature sizes of 0.25 μm and below has motivated the development of microlithography at the deep ultra-violet (DUV) laser wavelengths of 248 and 193 nm. In recent years the performance, reliability, and cost of ownership of excimer light sources have improved. Some key technologies needed for excimer lasers in microlithography include materials issues, gas lifetime, higher repetition rates and improved pulse-to-pulse energy repeatibility.

As dimensions of circuit elements shrink, new wavefront engineering technologies such as phase shifting techniques, off-axis illumination, and other modifications to extend the lifetime of optical lithography are required [1-5]. Simultaneous improvement of the resolvable linewidth (CD) and the depth of focus (DOF) is an important issue. Both CD and DOF are limited by the familiar scaling laws $CD = k_1\lambda/NA$ and $DOF = k_2\lambda/NA^2$, where λ is the wavelength and NA the numerical aperture of the projection lens. The parameter k_1 depends upon the imaging technology and process control, while k_2 has been within range of 1-2 for many years. The key innovations required for microlithography are those that reduce k_1. The 0.35 μm critical feature sizes required for the 64 Mb DRAM can be achieved with wavefront enhancement technology developed for i-line. Similarly, such techniques can be added to 248 nm DUV stepper systems to achieve the necessary resolution for 0.25 μm features needed for the production of the 256 Mb DRAM chip slated for initial production in 1998. The practical limit of optical lithography appears to be 0.12 μm required for the 4 Gb DRAM generation.

In 1987 Durnin [6] showed that the field described by $E(r,z,t) = A \cdot J_0(k_\perp r) \cdot e^{i(k_\parallel z - \omega t)}$ is an exact solution of the wave equation where $k_\perp^2 + k_\parallel^2 = \omega^2/c^2$, and J_0 is the zero-order Bessel function of the first kind. This field represents a nondiffracting beam, because the transverse intensity distribution is independent of the propagation distance z. However, such an ideal beam cannot be realized experimentally over large values of z and r, because the

SPIE Vol. 3092 • 0277-786X/97/$10.00

Downloaded From: https://www.spiedigitallibrary.org/conference-proceedings-of-spie on 2/22/2018 Terms of Use: https://www.spiedigitallibrary.org/terms-of-use

electric-field amplitude of the beam cannot be spatially integrated and would be rigorously exact only in infinite free space [6,8]. An experimental demonstration of a new method to generate nearly nondiffracting Bessel beams using a Fabry-Perot interferometer will be described. It was experimantally demonstrated that the DOF can be increased by a factor of 2 and simultaneously the transverse resolution improved by a factor of about 1.6, when using this technique to image contact holes.

2. Experiments and Results

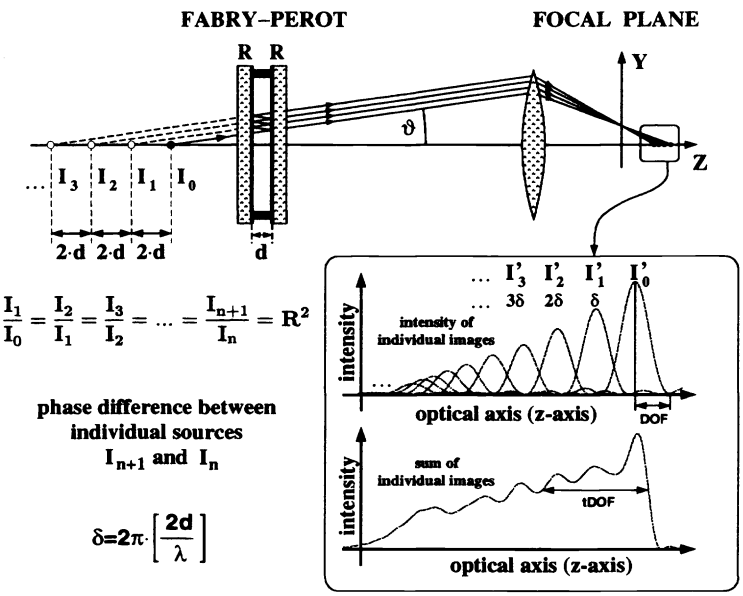

Figure 1: The image produced by the objective lens is the superposition of the images of the individual point sources.

Figure 1 shows the experimental arrangement used for generating nondiffracting Bessel beams. A point like source (I_0) generated by a microscope objective illuminates a scanning Fabry-Perot interferometer. Such a point like source plays the role of a contact hole on a mask. The aperture of the objective lens placed after the interferometer is adjusted so that it only transmits the first Fabry-Perot ring (at the rim of the aperture) and blocks all other rings. Due to multiple reflection in the interferometer, multiplied images (I_1, I_2, I_3 ...) of the only one real point like source will be obtained beyond I_0. The distance between these images is $2d$ and the intensity ratio is R^2 between adjacent individual sources where d is the separation and R is the reflectivity of the mirrors. The image produced by the objective is the superposition of the images of the individual point sources. The distance between these points is $2dM^2$, where M^2 is the longitudinal magnification of the objective lens. The intensity distribution on the optical axis strongly depends on the separation of the individual point like sources. It is possible to distinguish different cases depending on how many individual image points are in the range of one DOF. Let us define the relative image density (N) as

Downloaded From: https://www.spiedigitallibrary.org/conference-proceedings-of-spie on 2/22/2018 Terms of Use: https://www.spiedigitallibrary.org/terms-of-use

$$N = \frac{DOF}{2dM^2}. \tag{1}$$

N gives the number of image points in one DOF range. The image produced by the objective lens was magnified by two microscope objectives (the first was mounted on a precision translator to examine the axial intensity distribution) and monitored with a CCD camera (see Fig.2).

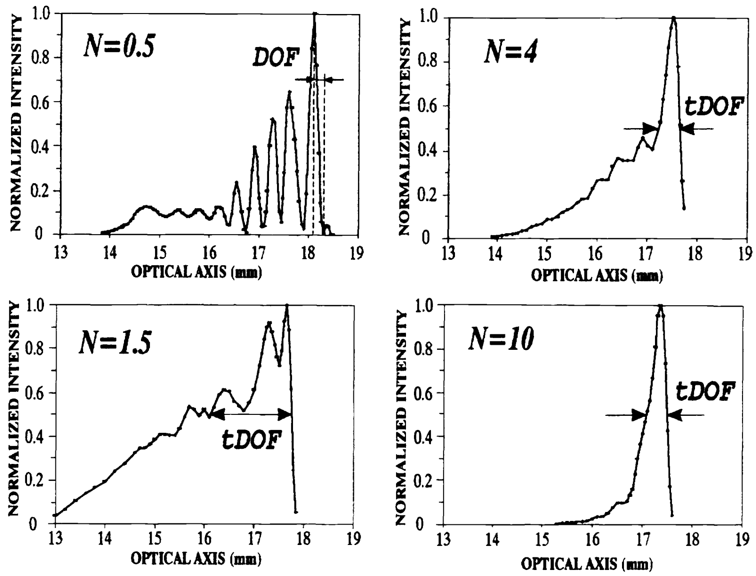

Figure 2: Measured intensity distribution on the optical axis for cases of different N values.

Four different experimental cases were studied ($N = 0.5$, 1.5, 4, and 10). In the first case ($N = 0.5$), the distance between the image points is twice the DOF, therefore the images can be observed separately. By decreasing the distance between the image points, the sharp peaks disappear and the intensity decreases faster on the optical axis. From a microlithographic point of view, oscillations in the intensity distribution are undesirable. By increasing the N ratio, the curves become smoother and the oscillations disappear. In the last case ($N = 10$), no oscillations occur. Since in case of superimposed images the first minimum is not zero, it is necessary to give a new definition of DOF so-called $tDOF$. $tDOF$ is defined as the range where the intensity is higher than the half of the main peak. The figures show normalized intensity, but in reality (due to the law of conservation of energy) by increasing the N ratio, the intensity of the main peak increases. The $N = 4$ case appears to be the optimum for microlithographic applications. The oscillations have already disappeared, and the $tDOF$ range is twice as large as without the Fabry-Perot interferometer.

The theoretically predicted intensity distribution in planes perpendicular to the optical axis is a J_0 function. The measured intensity distribution supports this prediction (Figure 3).

A comparison of the measured Bessel distribution and the Airy pattern showed that the FWHM of the Bessel beam is 1.6 times smaller than the FWHM of the Airy pattern. This decrease means an enhancement in the transverse resolution power.

Downloaded From: https://www.spiedigitallibrary.org/conference-proceedings-of-spie on 2/22/2018 Terms of Use: https://www.spiedigitallibrary.org/terms-of-use

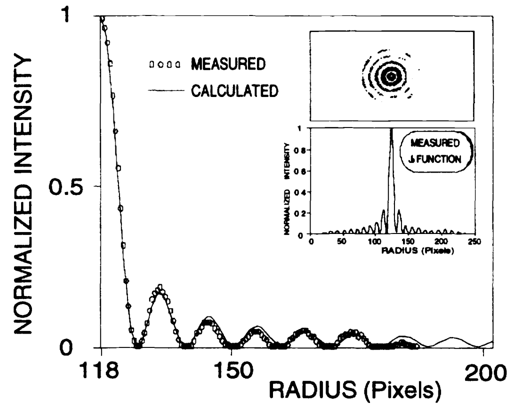

Figure 3: The measured intensity distribution perpendicular to the optical axis is quasi equivalent to a zero order Bessel function. The solid line shows the fitted curve to the measured intensity distribution (depicted by circles)

In microlithography it is often necessary to expose several contact holes simultaneously. To study the properties of imaging two contact holes (with special regard to the most critical case, when the first diffraction rings overlap), we placed a Michelson interferometer before the Fabry-Perot etalon. The experimental setup is shown in Figure 4.

The interferometer created two virtual point sources (P_1 and P_2) behind the mirror M_2. By slightly turning the mirrors M_1 and M_2, the relative transverse separation of P_1 and P_2 could be adjusted. Mirror M_1 was equipped with a PZT translator; thus, the relative phase difference between the virtual P_1 and P_2 could be arbitrarily adjusted. The inset of Figure 4 shows four different cases. In case a there is constructive interference between the first diffraction rings (the phase shift is 0), and the intensity between the two main peaks can reach 64%. Pictures b and c show intermediary cases, when the phase shift is in the range of 0 to π. In case d the phase difference is π and, due to the destructive interference, the intensity maximum between the main peaks is zero. These experiments, where the effect of a phase shift mask was simulated by a Michelson interferometer, show that even in the most critical case the undesirable effects of the interference of the diffraction rings can be considerably reduced with a phase shifting mask.

3. Discussions and Conclusions

Our experiments have demonstrated that for appropriate phase conditions the depth of focus could be increased significantly and that the transverse resolution improved by a factor of 1.6 when this technique is used to image isolated patterns such as contact holes. Although these experiments were performed with visible laser illumination, this method can be employed for I-line and deep UV lithography. For applications in a real optical stepper, further investigations are neccessary to determine the appropriate insertion point, reflectivity and thickness of the Fabry-Perot etalon. Insertion of a thin Fabry-Perot layer between the lens and the wafer has several advantages (e.g. separation of the images is independent of

Downloaded From: https://www.spiedigitallibrary.org/conference-proceedings-of-spie on 2/22/2018 Terms of Use: https://www.spiedigitallibrary.org/terms-of-use

the magnification), however scattering may decrease the image quality.

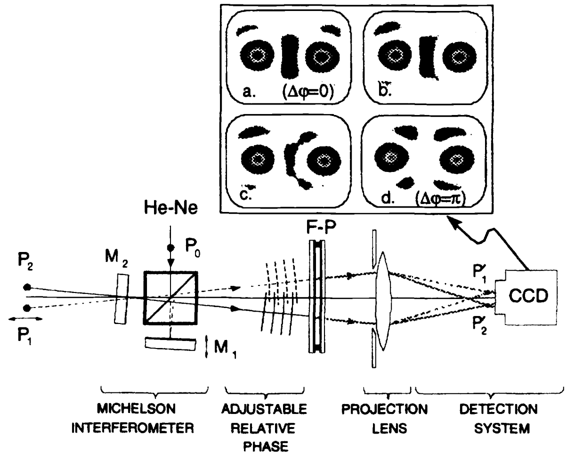

Figure 4: Imaging of two coherent point sources formed by a Michelson interferometer. The transverse distance and the relative phase difference between the sources was adjustable by translating and tilting the mirrors. The inset shows CCD images for different phase conditions.

Acknowledgment

This research was supported in part by Texas Instruments, NSF under grants DMI-9202639 and INT-9020541, and by the OTKA Foundation of Hungary (No. T20910).

References

1. M. D. Levenson, N. S. Viswanathan, and R. A. Simpson, *IEEE Trans. Electron Devices* **ED-29**, 1828 (1982).; M. D. Levenson, *Jpn. J. Appl. Phys* **33**, 6765 (1994).

2. H. Fukuda, N. Hasegawa and S. Okazaki, *J. Vac. Sci. Tech. B* **7(4)**, 667 (1989).

3. M. Erdélyi, Zs. Bor, J. R. Cavallaro, G. Szabó, W. L. Wilson, C. Sengupta, M. C. Smayling and F. K. Tittel, *Jpn. J. Appl. Phys.* **34**, L1629 (1995).

4. F. K. Tittel, M. Erdélyi, Zs. Bor, G. Szabó, J. R. Cavallaro, M. C. Smayling, and W. L. Wilson, in *Gas Lasers – Recent Developments and Future Prospects*, ed. W. J. Witteman and V. N. Ochkin, 263-272 (1996).

5. M. Erdélyi, Z. L. Horváth, G. Szabó, Zs. Bor, F. K. Tittel, J. R. Cavallaro and M. C. Smayling, Generation of Diffraction-Free Beams for Applications in Optical Microlithography (submitted to J. Vac. Sci. Tech. B)

6. J. Durnin, *J. Opt. Soc. Am.* **4**, 651 (1987).

7. J. Durnin, J. J. Miceli, Jr., and J. H. Eberly, *Phys. Rev. Lett.* **58**, 1499 (1987).

8. G. Indebetouw, *J. Opt. Soc. Am.* **6**, 150 (1989).

Downloaded From: https://www.spiedigitallibrary.org/conference-proceedings-of-spie on 2/22/2018 Terms of Use: https://www.spiedigitallibrary.org/terms-of-use